Growth and characterization of large high quality bownmillerite CaFeO2.5 single crystals

Growth and characterization of large high quality bownmillerite $CaFeO_{2.5}$ single crystals

Monica Ceretti, Andrea Piovano, Alain Cousson, Tanguy Berthier, Martin Meven, Giovanni Agostini, Jurg Schefer, Olivier Hernandez, Carlo Lamberti and Werner Paulus

CrystEngComm, **2012,** *14,* 5771–5776

DOI: 10.1039/c2ce25413a

Growth and characterization of large high quality bownmillerite $CaFeO_{2.5}$ single crystals

Monica Ceretti,[1,2] Andrea Piovano,[3,4] Alain Cousson,[5] Tanguy Berthier,[1,3] Martin Meven,[6] Giovanni Agostini,[3] Jurg Schefer,[7] Olivier Hernandez,[1] Carlo Lamberti[3] and Werner Paulus[1,2*]

The growth conditions of large and high quality single-crystal of CaFeO2.5 by the floating-zone technique in an image furnace are discussed. Structural characterization of the as grown single crystals have been carried out by neutron and X-ray diffraction as well as by HRTEM revealed the excellent quality in terms of composition homogeneity and crystalline quality. Magnetic measurements have been performed on oriented crystals by SQUID and neutron diffraction in the range of 5 – 700 K in order to clear up controversial discussions on possible magnetic phase transitions. Our results confirm the existence of a G-type antiferromagnetic ordering for the whole investigated temperature range. The magnetic transitions reported elsewhere are discussed in terms of oxygen non-stoichiometries leading to multiphase CaFeO2.5±δ related to the crystal growth conditions oriented crystals by SQUID and neutron diffraction in the range of 5 – 700 K in order to clear up controversial discussions on possible magnetic phase transitions. Our results confirm the existence of a G-type antiferromagnetic ordering for the whole investigated temperature range. The magnetic transitions reported elsewhere are discussed in terms of oxygen non-stoichiometries leading to multiphase $CaFeO_{2.5\pm\delta}$ related to the crystal growth conditions.

Introduction

The brownmillerite structure is known to be a deficient perovskite with the general formula $A_2BB'O_5$ where the B and B' cations adopt an octahedral and tetrahedral oxygen coordination, respectively. This structure can be deduced from the perovskite structure by introducing 1D chains of oxygen vacancies in the [110] direction with respect to the cubic perovskite structure, in a way that a superstructure with $a\sqrt{2} \otimes a\sqrt{2} \otimes 4a$ is formed. The brownmillerite structure consists thus of alternating $B'O_4$ tetrahedral layers and BO_6 octahedral layers along the $4a_{perov}$ axis. One important property found for some oxides with brownmillerite structure-type is their high oxygen ion mobility which might already present at ambient temperature.[1] Compounds like $SrFeO_{2.5}$ and $SrCoO_{2.5}$ can easily be oxidized by electrochemical oxidation or so called soft chemistry methods to obtain the respective $Sr(Fe,Co)O_3$ perovskite.[2-4] In this context it is rather surprising that $CaFeO_{2.5}$ equally showing the Brownmillerite type structure, cannot intercalate oxygen atoms using electrochemical oxidation and that $CaFeO_3$ can be obtained under drastic conditions only, e.g. at elevated temperature and high oxygen partial pressure.[5-8] In this sense the comparison of $CaFeO_{2.5}$ with $Sr(Fe,Co)O_{2.5}$ should provide valuable information for a general understanding of the high oxygen mobility at room temperature in the family of non-stoichiometric perovskites. The onset temperature for oxygen mobility to set in has been reported via $^{18}O/^{16}O$ isotope exchange to be 470°C for $CaFeO_{2.5}$, compared to 320°C for $SrFeO_{2.75}$.[9] In a recent study, the importance lattice dynamics may play for low temperature oxygen mobility in Brownmillerite type frameworks was evidenced. It was shown that oxygen diffusion mechanisms especially at moderate temperatures essentially rely on the existence of specific low energy lattice modes which trigger and amplify oxygen mobility in solids.[9] The concept to realize oxygen diffusion via lattice instabilities and dynamically triggered internal interfaces, was also shown to hold for oxides of the K_2NiF_4 type family,[10] offering a new dimension to design and to tune fast oxygen ion conductors in solids oxides but also more generally, for the understanding of low temperature solid state reactivity. Concerning compounds with Brownmillerite type frameworks, most of the studies were done on polycrystalline materials. The lack of single crystal studies on these non-stoichiometric oxides like $Sr(Fe,Co)O_{3-x}$ might be related to the formation of possible twinning domains, when coming from the high temperature perovskite structure with cubic symmetry to tetragonal or orthorhombic phases, and thus rendering structural studies complex.

The availability of single phase, high purity and large single crystals is, however, mandatory for detailed structural and lattice dynamical studies, but also to get more explicit information on the anisotropy of oxygen diffusion. The case is different for $CaFeO_{2.5}$, which is known to be stoichiometric under ambient oxygen partial pressure (i.e. 1 bar), at least up to 1200°C.

Since the high temperature symmetry of $CaFeO_{2.5}$ is still unknown, Krüger *et al.*[11,12] revealed for $CaFeO_{2.5}$ the existence of an incommensurate modulated structure with superspace group $Imma(00\gamma)s00$ and $\gamma = 0.5588$ at $T = 1100$ K, involving complex ordering of the $(FeO_4)_\infty$ chains within and also with the stacking of the tetrahedral layers along the *b* axis.[11] The phase transition from the incommensurate to commensurate phase also induces the formation of extended defects such as anti-phase boundaries, which have been interpreted to originate from a phase shift of the tilting sequence of the $(FeO_4)_\infty$ zigzag chains.[12] The influence of these lattice defects on oxygen mobility has not been considered in literature so far. Anisotropic oxygen mobility in $CaFeO_{2.5}$ has been recently reported for its low temperature reduction using CaH_2 applied on epitaxial thin films yielding $CaFeO_2$ with infinite layer structure.[13]

Another controversial point of $CaFeO_{2.5}$ concerns its magnetic properties, which are still matter of debate. $CaFeO_{2.5}$ has been reported to show G-type antiferromagnetic ordering with a Néel

temperature of 725 K.[14] However Marchukov *et al.*[15] found weak ferromagnetism resulting from the formation of Dzyaloshinskiy-Moriya domains and/or related to intergrowths or impurity phases. Maljuk *et al.*[16] argued that the weak ferromagnetism present in their $CaFeO_{2.5}$ crystals is not related to the presence of impurities. In the same reference they reported surprisingly on two new magnetic phase transitions at 140 K and 60 K which have not been observed so far and which remain of unknown origin. The authors claimed that both magnetic phase transitions should be intrinsically related to $CaFeO_{2.5}$.

Our efforts to dispose on large and high quality single crystals of $CaFeO_{2.5}$ goes consequently along with our motivation to study low temperature oxygen mobility in terms of anisotropic oxygen diffusion studied by the tracer method as well as the possible influence of lattice dynamics, but also to clear up the contradictory magnetic properties reported in literature so far. In this context the characterization of structure, lattice dynamics and magnetism especially using single crystals is of direct interest. Among the single-crystal growth techniques, the floating zone methods shows several advantages, e.g. the absence of impurities compared to methods using crucibles, as well as the possibility to obtain high quality single crystals of sufficiently large size for the characterizations mentioned above. We report here on $CaFeO_{2.5}$ single-crystal growth by the floating zone method and its structural characterization by neutron and X-ray diffraction as well as by HRTEM, completed by magnetic measurements on an oriented crystal using a SQUID and by neutron diffraction in the range of 5 – 700 K.

Experimental Section

Crystal growth.

Polycrystalline $CaFeO_{2.5}$ was prepared using standard solid-state chemistry methods. High purity $CaCO_3$ (99.95%) and Fe_2O_3 (99.99%) were thoroughly mixed and pressed into pellets of about 1 gram each. The pellets were then heated in air at 1000°C for 48 h. Calcination was repeated twice with intermediate grinding. Finally, the sample was annealed 1200°C for 24 h, followed by quenching from 1200°C in air down to ambient temperature. Seed and feed rods for crystal growth were obtained by hydrostatic pressing of $CaFeO_{2.5}$ powder at 10 bars in a cylindrical latex tube of 8 mm in diameter and 150 mm in length. The as obtained rods were then sintered in air at 1000°C for 24 h to obtain dense polycrystalline rods.

Single-crystal growth was carried out in an optical mirror furnace (NEC SC2, Japan) equipped with two 500 W halogen lamps as heat source and two ellipsoidal mirrors. Crystal growth was performed in air atmosphere with a typical traveling rate of 1-2mm/h, while the upper and lower shafts were rotated in opposite directions at 25 rpm. It is worth to note that $CaFeO_{2.5}$ melts congruently.

Crystal characterization

Several characterizations were performed on the as grown $CaFeO_{2.5}$ single crystal. Laboratory X-ray powder diffraction has been performed on a Bruker AXS D8 Advance diffractometer using Cu$K_{\alpha 1}$ radiation. The crystal quality and morphology has been checked by TEM analysis using a JEOL 3010-UHR HRTEM microscope operating at 300 kV, equipped with a 2k x 2k pixels Gatan US1000 CCD camera and with an OXFORD INCA EDS instrument for atomic recognition via X-ray fluorescence spectroscopy. The samples were deposited on a copper grid covered with a lacey carbon film. An ultramicrotome was used to section $CaFeO_{2.5}$ compound. A fragment of $CaFeO_{2.5}$ single crystal was oriented and encapsulated in a resin and then cut by means of a diamond blade in thin slices of material of about 60 nm of thickness. Slices of the as-cut sample were directly deposited on copper grid.

The bulk crystal quality, the nuclear and the magnetic structure were determined by neutron diffraction, performed on the four-circle diffractometers HEIDI[17-19] (FRM-II, München, λ = 0. 87 Å), 5C2[20] (LLB, CEA/Saclay, λ = 0.8302 Å) and TriCS[21] (PSI, Villingen, λ = 1.1767(1) Å).

Magnetisation studies of the as grown crystal was performed in a magnetic field (-5T ≤ H ≤ 5T) using a superconducting quantum interference device (SQUID) magnetometer MPMS (Quantum Design magnetic property measurement system) in the temperature range of 2–300 K.

Results and discussion

Structural investigations

Figure 1 shows a typically obtained $CaFeO_{2.5}$ single-crystal (CFO), 6 mm in diameter and 120 mm in length, showing a shiny, silver-black surface with metallic luster. All crystals were routinely checked for phase purity and inclusions by X-ray powder diffraction and SEM. Powder diffraction has been done on crashed parts of the as grown single crystals. A typical corresponding XRD pattern is shown in Figure 2. Pattern profile refinement carried out in the profile matching mode through the Fullprof software[22] and *Pnma* space group, shows a monophasic compound with the following lattice parameters: a = 5.4272(4), b = 14.7640(1) and c = 5.59724(4) Å, in a very good agreement with the values reported elsewhere.[9,14,23,24]

Fig. 1. As grown $CaFeO_{2.5}$ single crystal obtained by the floating zone method

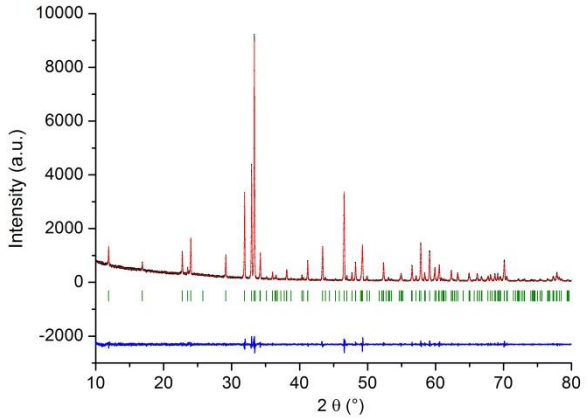

Fig. 2: Observed, calculated, and difference XRD (Bruker D8 Advance, Cuk 1) patterns of the as grown single CaFeO2.5 crystal in the Pnma space group, obtained in profile matching mode. Vertical bars are related to the calculated Bragg reflection positions.

The bulk crystalline quality of the as grown crystal has been checked on centimetre sized samples by neutron diffraction on the four-circle Heidi at FRM-II. Rocking curves measured in transversal ω-scan mode for several Bragg peaks are given in Figure 3. The FWHM of these profiles are close to the instrumental resolution for the whole diffraction range. We also investigated changes of the FWHM and integrated diffracted intensity as a function of the crystal orientation while turning the crystal around the scattering vector of the (101) plane (ψ-scan), the latter turned out to be the growth direction of all investigated crystals. The FWHM of the (202) reflection was found to show small but still significant variations over the angular range in ψ (see Fig. 1 supplementary information), going along with important variations of the integrated intensities. Since the used crystal was of cylindrical shape in the direction of the scattering vector, allowing to have constant absorption conditions for the whole ψ-scan range, the observed variation of intensity is consequently directly related to extinction effects only, i.e. to the anisotropy of the crystalline quality. In this context it is worth to note that the linear neutron true absorption coefficient for $CaFeO_{2.5}$ is weak and was calculated to be $\mu = 0.034$ cm $^{-1}$ at $\lambda = 0.87$ Å.

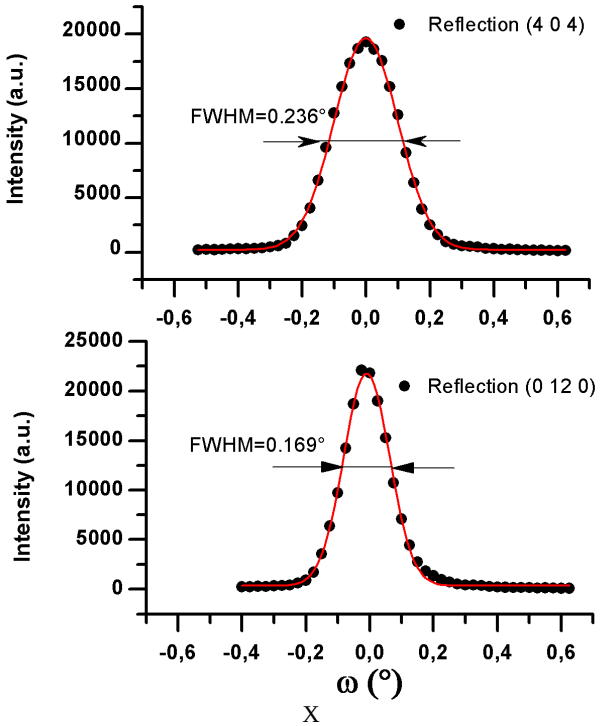

X

Fig. 3 Neutron rocking curve of the CFO single crystal (404) and (0 12 0) Bragg reflections, obtained on the four-circle Heidi[17-19] at FRM-II (λ = 0. 87 Å)

Figure 4 illustrates the evolution of the integrated intensity of the (202) reflection as a function of the ψ-angle, showing up to 50% variation of the integrated intensity with respect to its maximum value. The minimum position corresponds to a perfect alignment of the *b* axis, which is the stacking axis of octahedral and tetrahedral planes, within the plane of diffraction, spanned by the source, sample and point detector. This means that the mosaicity is most perfect when the (*a*,*c*) plane of the direct lattice is oriented perpendicular to the diffraction plane, and thus the orientation of the b-axis being in the diffraction plane. On the other hand the integrated intensity of the (202) reflection increases, when the (*a*,*c*) plane coincides with the diffraction plane, i.e. the b-axis pointing perpendicular to the diffraction plane. The extinction effect of the (202) reflection is thus strongly anisotropic and might be related to the presence of crystalline imperfections like micro-twinning and/or anti-phase domains related to the incommensurate-commensurate phase transition, as discussed by Krüger *et al.*[12]

To go further in the morphological characterization of the as grown $CaFeO_{2.5}$ single crystal, we used High Resolution Transmission Electron Microscopy (HRTEM). In fact, due to its ability to image a structure at local level, this technique is fundamental to elucidate ordering effects that cover a range of at maximum tenths of nm. It also should allow to detect the presence of anti-phase boundaries, as could be expected in the case of $CaFeO_{2.5}$ along the a-axis, as a possible consequence of a change of the tilting of the FeO_4 tetrahedra and/or FeO_6 octahedra.

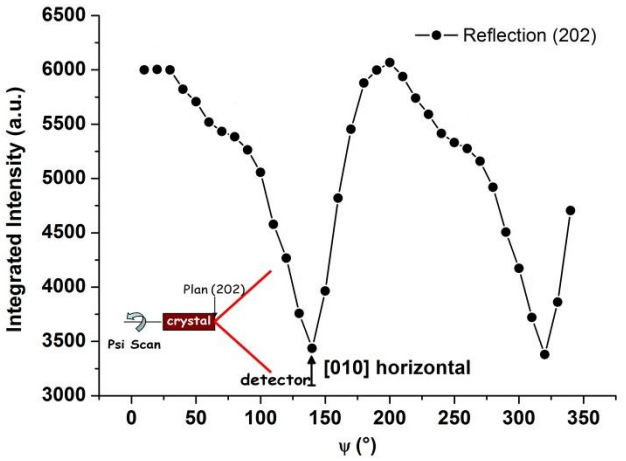

Fig. 4 Integrated intensities for the (202)-reflection, obtained via a Ψ-scan around the growth direction of the crystal corresponding to the [101]-axis

Figure 5 shows a high magnification image along [101] of a portion of $CaFeO_{2.5}$ sheet with high structural regularity, without any intergrowth regions. The contrast obtained by electrons phase interference from different zones of electron density constitute a regular pattern suggesting that, cell by cell, the position of atoms is not varied confirming as well the regularity of the stacking sequence of tetrahedral and octahedral layers in this structure. The Fourier Transform of HRTEM image gives the respective electron density map (see Figure 5), evidencing that the regular presence of darker almost-vertical stripes define the *b* axis of $CaFeO_{2.5}$. The measurement of axis length was performed averaging over 10 oscillations of electron density in the real image contrast, yielding a length of 14.76 Å. This value is in perfect accordance with the values found in X-Ray powder diffraction.

The elemental composition, checked by EDS on different slices of the single crystal, is homogeneous over the whole single crystal rod and, within the errors of the instruments, reflects the Ca:Fe:O stoichiometry 1:1:2.5 of the brownmillerite structure (Table 1).

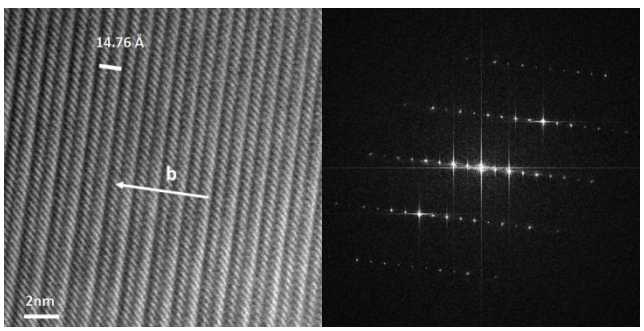

Fig. 5 HRTEM image of an extended ordered zone of $CaFeO_{2.5}$ single-crystal sheets obtained by microtome cut. The Fourier transform is shown on the right part.

We also checked the presence of anti-phase boundaries running parallel to [100] as reported by Krüger *et al.*[12] and which have been interpreted as a phase change of the orientation of the FeO_4 zigzag chains over the anti-phase boundary in [001], but were unable to visualize any. This might be related to the different synthesis conditions, which might strongly affect the microstructure. In ref. [12] a classical solid state reaction at high temperature was applied, while in our case the growth of a single crystal by the floating zone method was used. In addition to this we used the micro-slicing at low temperature, allowing to reduce any stress state which would be applied while grinding a polycrystalline material in a mortar. In this context it would be interesting to compare the appearance of anti-phase boundaries as a function of the sample preparation.

Nevertheless the drawback linked to any high-resolution imaging technique is related to the relatively small fraction of total volume sampled. Then we were unable to confirm local effects or distortions of the structure, within the statistic employed for the analysis. On the other hand, the presence or not of anti-phase boundary as discussed above may be related to method used for the sample synthesis: while the samples investigated by Krüger *et al.*[12] have been prepared by classical solid state reaction at high temperature, our crystals have been grown by the floating zone method. Furthermore all samples used for TEM study have been cut into thin slices by ultra-microtome.

Table 1. Summary of the elemental composition, checked by EDS and defining, within the experimental incertitude, the composition of as grown CaFeO2.5 single crystal.

Element	Weight %	Atomic %	Stoichiometry ratio
Ca	30.4±0.3	21.4	1
Fe	29.8±0.4	22.7	1
O	39.8±0.4	55.8	2.5

Summarizing, all these observations reveal the excellent quality of the as grown CFO single crystal in terms of mosaicity, absence of defects and c-staking faults and composition homogeneity.

Magnetic investigations

$CaFeO_{2.5}$ is well known to be an antiferromagnetic structure of G-type (T_N =725 K).[25-27] The room temperature nuclear and magnetic structure of $CaFeO_{2.5}$ has been refined from single crystal neutron diffraction data obtained for the as grown crystal on the four-circle neutron diffractometer 5C2 (LLB, CEA/Saclay). While the nuclear structure was refined in the *Pnma* space group, the magnetic structure was set up in the *Pn'm'a* by Geller *et al.*[27]

The refined magnetic moments values are M_x = 4.6(1) μ_B and M_x = -4.1 (1) μ_B respectively for the Fe(III) in octahedral and tetrahedral sites. They correspond to the values previously published by Takeda et al.[25] The results are summarized in Table 2.

Table 2. Structural parameters of as grown $CaFeO_{2.5}$ single crystal at room temperature. Results from neutron diffraction experiment (5C2, Saclay, λ=0.8302 Å). Average cell parameters: a = 5.430(2) Å, b = 14.76(2) Å and c = 5.601(4) Å, $\alpha = \beta = \gamma = 90°$. Average structure refined in *Pnma* space group from 897 independent reflections. R_F = 7.48 %, GoF=1.592. We want to state that the oxygen stoichiometry has been refined for all different sites in order to crosscheck for any non-stoichiometries. All O-sites showed a full occupation within an error bar of ±0.01

Atom	Site	x/*a*	y/*b*	z/*c*	oc	Uiso (Å^2)	Mx (μB)
Ca	*8d*	0.4834(2)	0.10758(5)	0.0265(2)	1	0.0080(1)	
Fe1	*4a*	0	0	0	0.5	0.0053(1)	4.6(1)
Fe2	*4c*	0.9427(2)	0.25	0.9325(2)	0.5	0.0054(1)	- 4.1(1)
O1	*8d*	0.2679(2)	0.98373(2)	0.2356(2)	1	0.0075(1)	
O2	*8d*	0.0256(3)	0.14015(3)	0.0748(2)	1	0.0097(1)	
O3	*4c*	0.0599(2)	0.25	0.8743(2)	0.5	0.057(3)	

In order to follow the reported magnetic phase transitions, we investigated the temperature dependence of two pure and strong magnetic reflections (120), (021) as well as one nuclear reflection (020), which have been measured from 5K up to the Néel temperature 725 K on the four circle diffractometers TriCS (5K < T < 300K) at SINQ and 5C2 (300K < T < 730 K) at the LLB. As it can be seen from Figure 6, the intensities of the magnetic reflections increase in a monotonous continuous way below T_N , which has been fitted to 700K, and reaches saturation at low temperature, while the nuclear one is constant over the whole temperature range. The (020) reflection has been chosen as standard reflection, as it is the less affected reflection for the Debye-Waller factor and is thus supposed to vary only slightly with T, since it appears at low momentum transfer of 0.068 sinθ/λ (Å^{-1}). From the changes of the intensities we deduce only one magnetic phase transition from the paramagnetic to antiferromagnetic state occurring at T_N = 700 K while no further anomalies could be found as described by Maljuk around 140K and 60K. We also performed additional magnetic measurements of the susceptibility on the same as grown CFO single crystal already used for neutron diffraction. Susceptibility measurements have been performed as a function of temperature but also varying an applied magnetic field (-5T<H<5T) along the *a* and *c* axes. In the following results are discussed for the applied field parallel to the c axis, i.e. the easy axis, and where the magnetic response of the sample is consequently higher as compared to the a-axis.

The thermal evolution of the magnetisation for the as grown CFO crystal (H//c) is shown in Figure 7. As shown from the neutron diffraction data in Fig 6, no anomalies have been evidenced that could indicate the onset of additional magnetic transitions, as pointed out by Maljuk *et al*.[16] The resulting small ferromagnetic component m_0 increases from 0.19 emu/g at room temperature up to 0.3 emu/g at 2K and is related to a canting of all magnetic moments towards the c-direction.

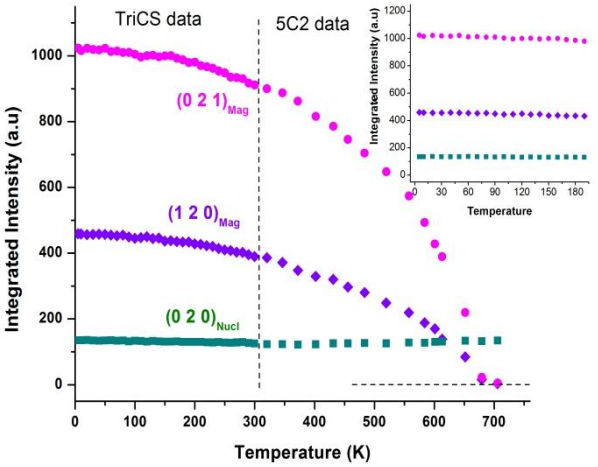

Fig. 6. Evolution of the integrated intensity as a function of the temperature of the purely magnetic reflections $(0\ 2\ 1)_{Mag}$ and $(1\ 2\ 0)_{Mag}$, as well as of purely nuclear $(0\ 2\ 0)_{Nucl}$ one. The inset shows a magnification of the low temperature region.

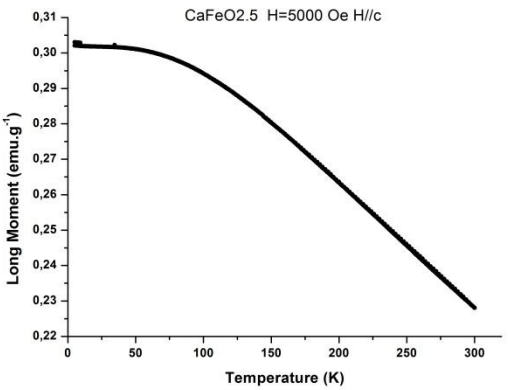

Fig. 7. Magnetization of the as-grown CFO single crystal with temperature, under an applied magnetic field of 5000 Oe parallel to the *c*-axis.

Figure 8 shows the isothermal magnetisation curves with the magnetic field applied along the c axis at different temperatures (2K, 5K, 20K and 300K). For temperatures above 5 K the magnetisation becomes zero if no field is applied.

While for 5K, 20 K and 300 K magnetism comes down close to zero in the absence of an external magnetic field, the 2 K data show a non-zero value. This magnetic phase transition has not been reported so far and is currently under investigation. The absence of a ferromagnetic component at 20K has been proven by magnetization measurements with the crystal orientation along the c-axis. No hysteresis has been detected, suggesting no changes in the AF orientation of the magnetic moments down to this temperature.

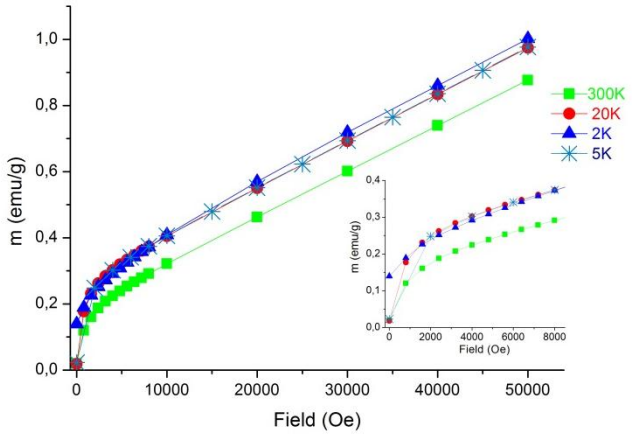

Fig. 8 Magnetisation isotherms for the as grown CFO crystal (H//c) measured up to a field of 55kOe at selected temperatures of 2K, 5K, 20K and 300K. The inset shows the details of the low field magnetization process

Conclusions

High quality single-crystal of $CaFeO_{2.5}$ has been grown with the help of a mirror furnace, using the floating zone. The optimized growth parameters allowed to obtain large and homogeneous crystals without significant mosaic spread and stacking faults along the octahedral and tetrahedral layer sequence. We also evidenced the absence of any anti phase boundaries related to the incommensurate-commensurate phase transition as reported by Kruger *et al.*[11,12] on samples obtained by classical solid-state synthesis. In this way one may wonder whether the synthesis conditions play a predominant role for the existence or not of these types of extended defects. In the same context is surprising to note the general absence of twin domains even for large $CaFeO_{2.5}$ single crystals, as one would expect in case of a cubic/orthorhombic phase transition, and which is the case for the homologous $SrFeO_{2.5}$ or $SrCoO_{2.5}$, where the high temperature parent phases are indeed of cubic symmetry. This suggests the absence of any phase transition in $CaFeO_{2.5}$ towards high temperatures up to the melting temperature, with the exception of the commensurate-incommensurate transition. This also holds for a possible tetragonal/orthorhombic phase transition in view of the similarity of the a- and c-axis lattice parameters. The absence of a phase transition might be related to the relatively short b-lattice parameter of 14.76 Å, compared to 15.57 Å for the homologous $SrFeO_{2.5}$, which puts the tilting dynamics of the 1D-$(FeO_4)_\infty$ tetrahedral chains for $CaFeO_{2.5}$ on a deeper potential, avoiding a transition towards a cubic and oxygen deficient phase with perovskite structure.

The high quality of the crystal has also been confirmed by magnetic measurements, since we were able to approve the G-type magnetic structure as suggested by earlier studies. The magnetic phase transitions found by Maljuk et al. on $CaFeO_{2.5}$ single crystals, are thus supposed to have a different origin.[16] Beside phase impurities or segregation effects one may also discuss a slight modulation of the oxygen stoichiometry, since the crystal reported here has been obtained in air, while Maljuk et al. reported the growth conditions under 1-2 bar of oxygen. Contrary as one might expect from the different oxygen partial pressures, the oxygen stoichiometry given in the work of Maljuk *et al.*[16] corresponds to $CaFeO_{2.96\pm0.04}$ while the structural characterization undertaken by single crystal neutron diffraction reported here, yields a stoichiometric oxygen composition of $CaFeO_{2.5}$ within the error bars. On the other hand we want to point out some inconsistencies of the XPD-pattern given in ref. [16], as some reflections seem to be splitted, which is the case e.g. for the (011) and (002), and/or show a strong asymmetry towards lower diffraction angles, which cannot be explained by $K_{\alpha 12}$ splitting. This concerns especially reflections where the c-axis is involved, which supports the above-mentioned idea of a non-homogenous oxygen stoichiometry and related phase separation, obviously present for a narrow stoichiometric range. This phenomenon is presently under investigation.

Acknowledgements

T. Guizouarn from “Mesures Physiques” - Sciences Chimiques de Rennes - is acknowledged for the magnetic measurements. The authors also thank “Rennes Metropole” for financial support. This collaboration has been realized inside the frame of the consortium of the EMMC MaMaSELF (www.mamaself.eu). We acknowledge the use of neutron beam time on 5C2 at the LLB, HEIDI at FRMII and TriCS at SINQ

Notes and references

[1] *Sciences Chimiques de Rennes, UMR 6226 CNRS-Université de Rennes1, Inorganic Materials: Soft Chemistry and Reactivity of Solids, Bât. 10B, Campus de Beaulieu, F-35042 Rennes, France*
[2] *University of Montpellier 2, UMR 5253, ICGM, C2M, CC1504, 5 Place Eugène Batallion, F-34095 Montpellier, France*
[3] *Department of Chemistry, NIS Center of Excellence, and INSTM unit, University of Turin, Via Giuria 7, I-10125 Turin, Italy*
[4] *Institut Laue-Langevin (ILL), BP 156 X, F-38042 Grenoble Cedex, France,*
[5] *LLB, CEA/Saclay 91191 Gif-sur-Yvette cedex, France*
[6] *TU-München, FRM-II, München, Germany*
[7] *Laboratory for Neutron Scattering Paul Scherrer Institut, CH-5232 Villigen PSI, Switzerland*
* To whom the correspondence should be addressed. E-mail: werner.paulus@univ-montp2.fr.
Electronic Supplementary Information (ESI) available: [Figure showing the evolution of the FWHM of the (202) and (404) reflections as a function of the Ψ angle]. See DOI: 10.1039/b000000x/

1 M. V. Patrakeev, I. A. Leonidov, V. L. Kozhevnikov and V. Kharton, *Solid State Sci.*, 2004, **6**, 907.

2 A. Nemudry, E. L. Goldberg, M. Aguirre and M. A. Alario-Franco, *Solid State Sci.*, 2002, **4**, 677.

3 R. Le Toquin, W. Paulus, A. Cousson, C. Prestipino and C. Lamberti, *J. Am. Chem. Soc.*, 2006, **128**, 13161.

4 A. Piovano, G. Agostini, A. I. Frenkel, T. Bertier, C. Prestipino, M. Ceretti, W. Paulus and C. Lamberti, *J. Phys. Chem. C*, 2011, **115**, 1311.

5 F. Kanamaru, H. Miyamoto, Y. Mimura, M. Koizumi, M. Shimada, S. Kume and S. Shin, *Mater. Res. Bull.*, 1970, **5**, 257.

6 T. Takada, R. Kanno, Y. Kawamoto, M. Takano, S. Kawasaki, T. Kamiyama and F. Izumi, *Solid State Sci.*, 2000, **2**, 673.

7 T. Saha-Dasgupta, Z. S. Popovic and S. Satpathy, *Phys. Rev. B*, 2005, **72**, Art. N. 045143.

8 A. L. Shaula, Y. V. Pivak, J. C. Waerenborgh, P. Gaczynski, A. A. Yaremchenko and V. V. Kharton, *Solid State Ion.*, 2006, **177**, 2923.

9 W. Paulus, H. Schober, S. Eibl, M. Johnson, T. Berthier, O. Hernandez, M. Ceretti, M. Plazanet, K. Conder and C. Lamberti, *J. Am. Chem. Soc.*, 2008, **130**, 16080.

10 A. Villesuzanne, W. Paulus, A. Cousson, S. Hosoya, L. Le Dreau, O. Hernandez, C. Prestipino, M. I. Houchati and J. Schefer, *J. Solid State Electrochem.*, 2011, **15**, 357.

11 H. Krüger and V. Kahlenberg, *Acta Crystallogr. Sect. B-Struct. Sci.*, 2005, **61**, 656.

12 H. Krüger, V. Kahlenberg, V. Petrícek, F. Phillipp and W. Wertl, *J. Solid State Chem.*, 2009, **182**, 1515.

13 S. Inue, M. Kawai, N. Ichicawa, H. Kageyama, W. Paulus and Y. Shimakawa, *Nat. Chem.*, 2010, **2**, 213.

14 P. Berastegui, S. G. Eriksson and S. Hull, *Mater. Res. Bull.*, 1999, **34**, 303.

15 P. Marchukov, R. Geick, C. Brotzeller, W. Treutmann, E. G. Rudashevsky and A. M. Balbashov, *Phys. Rev. B*, 1993, **48**, 13538.

16 A. Maljuk, J. Strempfer and C. T. Lin, *J. Cryst. Growth*, 2003, **258**, 435.

17 V. Hutanu, M. Meven and G. Heger, *Physica B*, 2007, **397**, 135.

18 V. Hutanu, M. Meven, E. Lelievre-Berna and G. Heger, *Physica B*, 2009, **404**, 2633.

19 V. Hutanu, M. Janoschek, M. Meven, P. Boni and G. Heger, *Nucl. Instrum. Methods Phys. Res. A*, 2009, **612**, 155.

20 The technical data sheet for the 5C-2 hot neutron four-circle diffractometer at LLB, CEA (Saclay) can be found at http://www-llb.cea.fr/en/fr-en/spectro/5c2/5c2.html.

21 J. Schefer, M. Konnecke, A. Murasik, A. Czopnik, T. Strassle, P. Keller and N. Schlumpf, *Physica B*, 2000, **276**, 168.

22 J. Rodríguez-Carvajal, *IUCr Newsletter*, 2001, **26**, 12_19. The complete FULLPROF suite can be obtained from: http://www.ill.eu/sites/fullprof/index.html.

23 T. Berthier, *joint PhD Thesis in Materials Science, University of Turin and of Rennes-1*, 2007.

24 A. Piovano, *joint PhD Thesis in Materials Science, University of Turin and of Rennes-1*, 2011.

25 T. Takeda, Y. Yamaguchi, S. Tomiyoshi, M. Fukase, M. Sugimoto and H. Watanabe, *J. Phys. Soc. Jpn.*, 1968, **24**, 446.

26 P. D. Battle, T. C. Gibb and P. Lightfoot, *J. Solid State Chem.*, 1988, **76**, 334.

27 S. Geller, R. W. Grant, U. Gonser, H. Wiedersich and G. P. Espinosa, *Phys. Lett. A*, 1967, **25**, 722.